HiSST: 2nd International Conference on
High-Speed Vehicle Science Technology
11–15 September 2022, Bruges, Belgium

Testing and Characterization of Near-Zero-Ablation Fibre-reinforced Ultra High Temperature Ceramics for Aerospace

Stefano Mungiguerra[1], Giuseppe D. Di Martino[2], Anselmo Cecere[3], Raffaele Savino[4], Diletta Sciti[5]

Abstract

This paper presents the results of extensive test campaigns carried out in the framework of the European C^{3}HARME project, for the characterization of Ultra-High-Temperature Ceramic Composites for near-zero ablation Thermal Protection Systems (TPS) and near-zero erosion rocket nozzles. Tests were carried out in a supersonic arc-jet wind tunnel, where conditions typical of atmospheric re-entry were reproduced, and in different configurations in a lab-scale hybrid rocket engine. Materials having a ZrB_2-SiC-based matrix and carbon fibre reinforcement showed an outstanding erosion resistance for both applications. In the arc-jet environment, a spontaneous temperature jump of 4-500 K was observed, which was attributed to a combination of increased catalytic activity and reduced thermal conductivity upon oxidation. In the high-pressure environment of the propulsion tests, long-fibre reinforcement demonstrated better mechanical resistance, which can be improved by proper tuning of the densification process. The small-scale results paved the way for large scale qualification tests on a complete TPS assembly and a medium-scale solid rocket nozzle.

Keywords *Ultra-High-Temperature Ceramic Matrix Composites, Arc-jet testing, Hybrid rocket nozzles*

Nomenclature (Tahoma 11 pt, bold)

Latin
H_0 – Specific total enthalpy
T – Temperature
p – Pressure

Greek
ε_λ – Surface spectral emittance

1. Introduction

The extremely demanding aero-thermo-dynamic conditions encountered by hypersonic vehicles during atmospheric re-entry make the design of proper Thermal Protection Systems (TPS) a topic of utmost importance, requiring continuous improvement of materials and technologies [1, 2]. The environment of re-entry includes hypersonic Mach numbers, projected service temperatures above 2000°C or recombination reactions of dissociated gases which can substantially enhance the heat flux on the exposed surface of the spacecraft [3, 4].

[1] *University of Naples "Federico II", Department of Industrial Engineering, Aerospace Division, P.le Tecchio 80, 80125 Napoli, Italy, stefano.mungiguerra@unina.it*
[2] *University of Naples "Federico II", Department of Industrial Engineering, Aerospace Division, P.le Tecchio 80, 80125 Napoli, Italy, giuseppedaniele.dimartino@unina.it*
[3] *University of Naples "Federico II", Department of Industrial Engineering, Aerospace Division, P.le Tecchio 80, 80125 Napoli, Italy, anselmo.cecere@unina.it*
[4] *University of Naples "Federico II", Department of Industrial Engineering, Aerospace Division, P.le Tecchio 80, 80125 Napoli, Italy, raffaele.savino@unina.it*
[5] *National Research Council of Italy, Institute of Science and Technology for Ceramics, Via Granarolo 64, 48018 Faenza, Italy, diletta.sciti@istec.cnr.it*

On the other hand, challenges for solid and hybrid rocket technologies include the design and fabrication of non-eroding firing thrusters able to survive severe thermal-structural and thermal-chemical combustion environments without cooling systems. The inner surface of the exhaust nozzle, through which the propellant flow is accelerated to supersonic conditions, is very critical in this sense, as it is subjected to the highest shear stresses, pressure and heat fluxes in a chemically aggressive environment. These severe conditions usually lead to removal of surface material (ablation) due to heterogeneous reactions between oxidizing species in the hot gas and the solid wall [5]. Because of the material erosion, there is an enlargement of the nozzle throat section and a consequent decrease of the rocket thrust, with detrimental effects over the motor operation. Thus, the requirement that dimensional stability of the nozzle throat should be maintained makes the selection of suitable rocket nozzle materials extremely hard [1].

The materials used for ultra-high-temperature aerospace applications include refractory metals, refractory metal carbides, graphite, ceramics and fibre-reinforced plastics [6, 7]. At present, silicon-based ceramics such as silicon carbide (SiC) and coated carbon-carbon (C-C) composites are the most widely employed solutions for TPS of re-entry vehicles, but they are only able to withstand temperatures up to ~2000K [8, 9]. For rocket nozzles, certain classes of materials demonstrated superior performances under specific operating conditions but the choice depends on the specific application. For instance, fully densified refractory-metal nozzles generally are more resistant to erosion and thermal-stress cracking than the other materials. Graphite performs well with the least oxidizing propellant but is generally eroded severely [10].

Ultra-High-Temperature Ceramic (UHTC) composites, based on transition metal borides, carbides, and nitrides, are considered promising candidate materials for the considered applications due to their melting temperatures that exceed 3250K, and good strength and oxidation resistance over 2250K [11, 12]. High oxidation rates and poor mechanical properties limit the applicability of single phase materials. Silicon carbide or other silicon-based phases, as particles, whiskers, or short fibres, are frequently added to improve oxidation resistance and damage tolerance [13-15]. To further increase fracture toughness and thermal shock resistance, research is currently oriented towards carbon fibre reinforced UHTC-matrix composites (UHTCMC) with the aim of developing ultra-refractory components with enhanced mechanical properties and reliability [16].

Within this framework, the University of Naples "Federico II" (UNINA) and the Institute of Science and Technology for Ceramics of the National Research Council of Italy (ISTEC-CNR) have been involved in the Horizon 2020 European C^{3}HARME research project [17], which is focused on a new class of UHTCMCs for near zero-erosion rocket nozzles and near zero-ablation TPS. Extensive experimental campaigns were carried out for the characterization of sintered ZrB_2-based ceramics reinforced with carbon fibres, based on an incremental approach, envisaging tests on prototypes of increasing complexity [4]. The experiments were always complemented by Computational Fluid Dynamics (CFD) simulations to provide a deeper understanding of the observed phenomena and a complete characterization of the test conditions. This paper summarizes all the experimental activities performed at UNINA for both the applications and the main scientific and technological outcomes of the test campaigns.

2. Experimental facilities

2.1. SPES arc-jet wind tunnel

SPES (Small Planetary Entry Simulator, Fig. 1a) is a continuous, open-circuit, blow-down arc-jet wind tunnel, provided with a torch (Perkin-Elmer 9MB-M) with maximum power of 80 kW, able to operate with inert gas (He, N_2, Ar and their mixtures), which is connected, downstream, to a mixing chamber and then to a conical convergent/divergent nozzle exhausting into the test chamber where pressure is lowered by two vacuum pumps in series, a mechanical booster (EH4200) and radial pump (E2M275). This vacuum system is able to achieve a static pressure of 10 Pa in the test chamber. The torch, the mix-chamber and the nozzle are cooled by water flowing in a double wall. A nitrogen plasma is generated by the industrial torch at mass flow rates up to 5 g/s. In order to simulate the air composition, the mixer downstream the torch is used to supply a secondary gas (e.g. O_2) to the primary plasma. Specific total enthalpies above 20 MJ/kg are achieved at gas mass flow rate of 1g/s. The convergent-divergent conical nozzle is characterized by a throat diameter of 11 mm, and an outlet diameter of 22 mm and is able to accelerate the flow up to a nominal Mach number about 3.

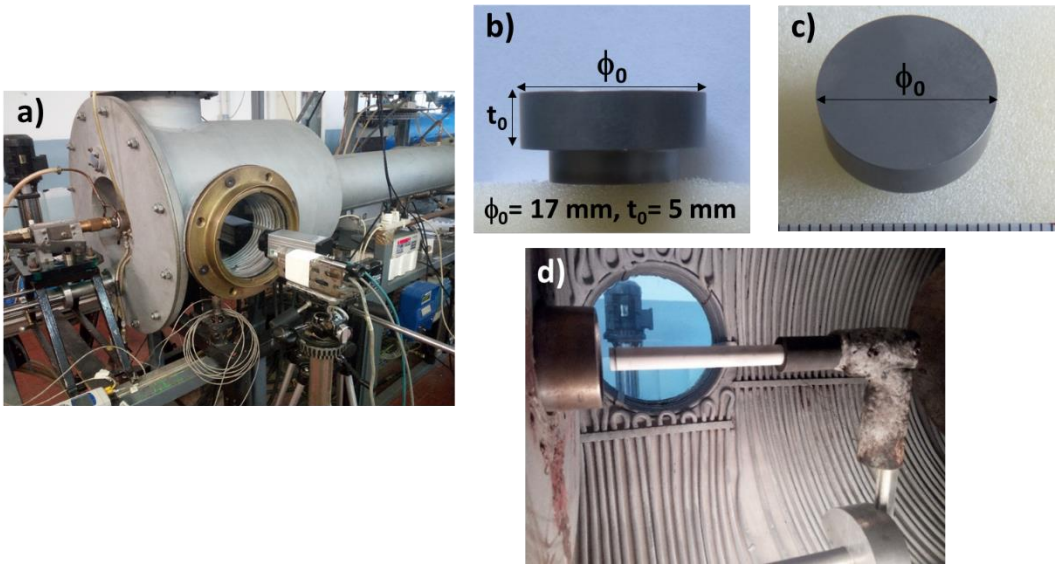

Fig. 1. a) SPES arc-jet wind tunnel, b-c) nominal geometry of test samples, d) samples mounted inside the test chamber

The test articles (nominal design in Fig. 1b,c) were accommodated inside the test chamber of the plasma wind tunnel, at the exit of the supersonic nozzle, by using a dedicated set-up with thermally protected mechanical supports (Fig. 1d). The position was regulated to place the sample at the desired distance from the nozzle. In the current test campaigns, the samples were placed at a distance of 1 cm from the nozzle.

Samples were exposed to a supersonic flow generated by the expansion of a high enthalpy gas mixture of nitrogen (0.8 g/s) and oxygen (0.2 g/s). During the test, the arc power of the plasma torch and consequently the total enthalpy of the flow were gradually increased through successive increments, leading correspondingly to an increase of pressure and temperature. A quasi-stationary condition generally occurs when the maximum value of temperature is reached during the last steps of the test. In the tests discussed in the present paper, the nominal duration of each step was 30 seconds, except for the last step of 120 seconds. The total specific enthalpy (H_0) is obtained through an energy balance at the exit of the plasma torch, based on measurement of temperature and flow rate of cooling water.

In Table 1, the typical values of the physical quantities of interest for each torch arc power step are reported. Specific total enthalpy values are averaged over different test, with an uncertainty around ±1 MJ/kg. Heat fluxes were measured by a copper slug calorimeter. The pressure in the test chamber was approximately equal to 2 mbar. At the end of the most stressful enthalpy step, the torch power was decreased gradually until facility shutdown, resulting in a stepwise cooling of the buttons.

Table 1. Test conditions in SPES facility

Step	H_0 [MJ/kg]	Heat Flux - Slug Calorimeter [MW/m^2]	Stagnation Point Pressure [mbar]
0	5.5	0.8	62
1	7.0	0.95	64
2	8.5	1.1	67
3	10	1.5	70
4	12	2.0	73
5	14	2.5	76
6	16	3.0	79
7	18	3.6	82
8	20	4.2	85

The surface temperature of the samples was continuously measured (±1% instrumental accuracy) by digital two-colour pyrometers (Infratherm ISQ5 and IGAR6, Impac Electronic GmbH, Germany) at an acquisition rate of 100 Hz. In addition, the infrared response of the specimen during the arc-jet testing was obtained by means of an infrared (IR) thermo-camera (TC, Pyroview 512N, DIAS Infrared GmbH, Germany). The two-colour ISQ5 pyrometer exploits two overlapping infrared wavelength bands at 0.7–1.15 μm and 0.97–1.15 μm to measure the temperature from 1273 K up to 3273 K. The IGAR6 pyrometer operates in the bands 1.5-1.6 μm and 2.0-2.5 μm to return the sample temperature in the range 523-2273 K. The measurement area of the ISQ5 pyrometer is approximately a round spot 3.3 mm in diameter. The pyrometers mode can be set in order to give back the peak value of the temperature field detected inside the focused area. In addition, the so-called "two-colour mode" provides an output value independent on the (directional) spectral emittance (ε_λ). It is generally assumed that the observed surface behaves as a grey body over the operating temperature range. Surface chemical reactions occurring during testing can have been responsible for changes in ε_λ versus testing time. On one hand, the two-colour pyrometers overcome this problem measuring the true temperature. On the other hand, the IR-TC detects the spectral radiance coming out from the heated sample along the infrared band wavelength of 0.8-1.1 μm. The surface temperature distribution can be calculated assuming constant emissivity along the monitored surfaces of the samples and taking into account the axial symmetry of the specimens. Once the local temperature was measured thanks to the pyrometers at the measurement spot, that value was input to determine the spectral emittance in the range of the IR-TC, and finally the surface temperature distribution was evaluated. The operating wavelength is that in which most of the radiative power is emitted at ultra-high temperatures [69], which reduces the error in temperature estimation due to spectral emittance uncertainty (an error of 10% in emissivity leads to an error of about 1% in temperature). High-Definition videos of the tests were recorded by means of a Camera Flea3 1.3 MP Color USB3 Vision with a resolution of 1328x1048 and a frame rate equal to 25 fps. A picture of the optical and infrared setup in shown in **Error! Reference source not found.**.

A balance (1 mg accuracy) and a precision calliper (0.01 mm accuracy) were used to measure mass and thickness losses of the specimen. In the post-processing analyses, two erosion rates were calculated: one based on the loss of mass (assuming uniform consumption of the sample in the axial direction) and the other evaluated by the thickness measurement made by the calliper.

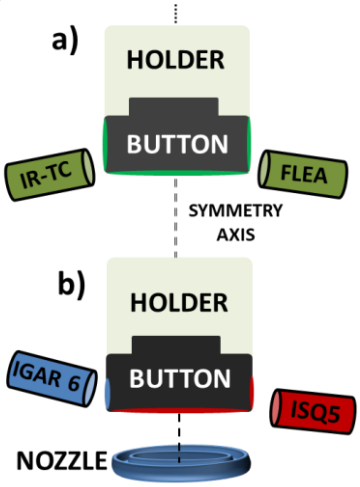

Fig. 2. Arrangement of pyrometers ISQ5 and IGAR6 (a), and infrared (IR) thermo-camera (TC) with video recorder FLEA (b): the coloured portions of the button surface match diagnostics and their field of view.

2.2. Aerospace Propulsion Laboratory

The experimental activities presented in this work for the characterization of materials for rocket nozzles have been carried out at UNINA Aerospace Propulsion Laboratory. The test rig is a versatile set up primarily designed for testing hybrid rocket engines of several sizes and its sub-components. A detailed description of the laboratory and of the experimental facilities can be found in Ref. [18].

For the current research activities, novel, dedicated test set-ups were developed to test the new high-performance UHTCMC materials in different configurations. Fig. 3 shows the design of the different proposed test articles. In particular, a first test campaign has been already successfully carried out to screen the most suitable materials candidates for the final applications, exposing small UHTCMC specimens (same size as for SPES tests, see previous section) to the supersonic exhaust jet of a 200N-class hybrid rocket nozzle [19, 20]. Based on these preliminary results, flat disks to be placed inside the hybrid rocket combustion chamber were manufactured and tested to assess the capability of larger components to withstand the considerable thermo-mechanical stresses expected inside the rocket without significant erosion. Then, nozzle-throat inserts and complete UHTCMC nozzles were tested to validate the technologies on samples having a shape and dimension close to the final application.

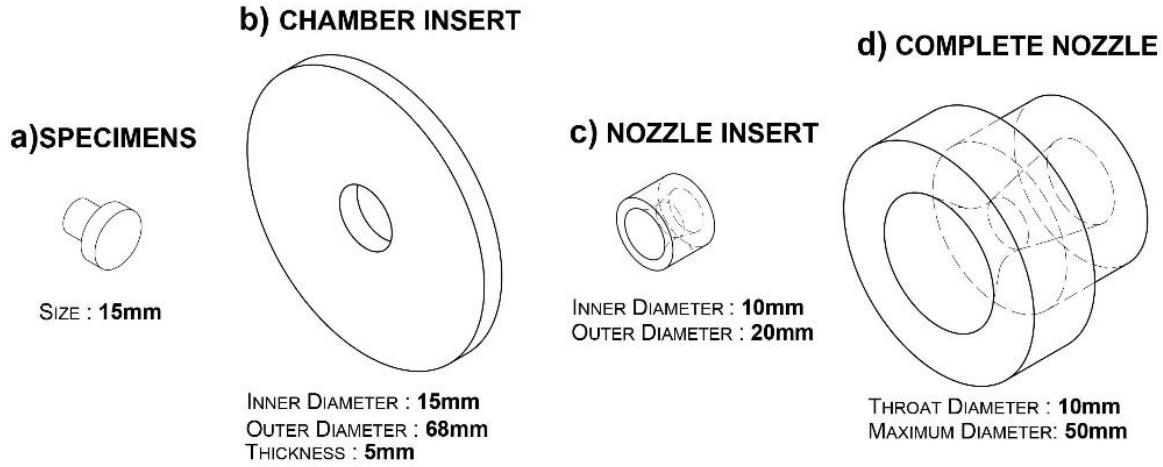

Fig. 3. Design of the test articles for material characterization for Hybrid Rocket Propulsion application.

The schematics of the rocket employed in this work is depicted in Fig. 4, which also shows the UHTCMC sample (in blue) behind the rocket nozzle, the possible configuration for the chamber insert (in red) and the position of the nozzle. The tests presented in the following sections were performed with a converging nozzle injector, whose exit-section diameter is 6 mm, which delivered oxygen in single-port cylindrical fuel grains of HDPE. Oxidizer mass flow rate is controlled by means of a Tescom ER3000 pressure regulator, which controls an electropneumatic valve in order to reduce the feeding pressure to the desired setpoint, upstream a chocked Venturi nozzle. The average fuel mass flow rate is estimated by means of grain mass measurements before and after the test (see Ref. [21]). Chamber pressure is measured by two capacitive transducers, Setra model C206, set up in the prechamber and in the aft-mixing chamber, while four load cells installed on the test bench allow thrust measurements. Finally, non-intrusive diagnostic equipment employed for the real-time evaluation of the sample surface temperature. In particular, the surface temperature of the samples can be continuously measured (±1% instrumental accuracy) by digital two-color pyrometers (Infratherm ISQ5 and IGAR6, Impac Electronic GmbH, Germany) at an acquisition rate of 100 Hz.

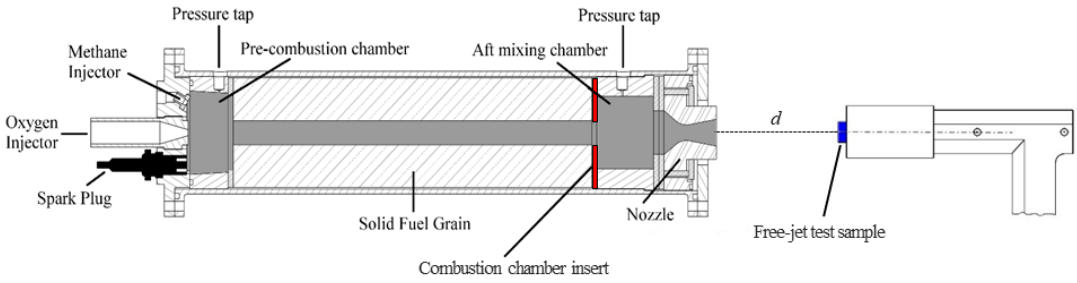

Fig. 4. Layout of 200 N-class hybrid rocket engine, including the set-up for UHTCMC testing.

Different test conditions have been selected, to evaluate the materials performance in different aero-thermo-chemical environments. Tests had a nominal duration of 10 or 15 s. Cylindrical 220mm-long

HDPE grains were employed as fuel and gaseous oxygen as oxidizer, at different mass flow rate (25, 30 or 40 g/s). Heat fluxes on the order of 10-15 MW/m^2 were achieved, which are well representative of a real rocket application.

3. Results

3.1. UHTCMC for Thermal Protection Systems

The arc-jet tests described in this section allowed comparing the behaviour of different UHTCMC formulations, having different matrix compositions and long- of short-carbon fibre reinforcement. Fig. 5 shows a comparison among the ablation rates (based on mass loss) of the samples. Four tests on graphite are shown as a reference. Samples Graphite_1 and Graphite_3 were tested at conditions corresponding to step #0 (H_0 = 5.5 MJ/kg). Samples Graphite_2 and Graphite_4 were tested at conditions corresponding to steps #1-3 (at H_0 up to 10 MJ/kg).

ZrB_2-based samples showed an outstanding ablation resistance, although experiencing a sudden rise in temperature (*temperature jump*) of several hundred degrees, reaching temperatures up to 2700-2800 K. As shown in Fig. 6 (which is referred to a long-fibre ZrB_2-SiC-based sample, as an example), the *temperature* jump occurred only on the front surface of the specimens, while the rear part remained at relatively lower temperature. These samples develop a ZrO_2 solid coating preventing consistent sample erosion, especially at ultra-high temperature, when the oxide melts and form a dense scale; however, after exposure to plasma flow and *temperature jump*, the thin oxide layer is characterized by poor mechanical properties, rather compact but in some cases partially detached from the underneath boride matrix (Fig. 7). Moreover, even in presence of a *temperature jump*, the low thermal conductivity of oxide phases appears to shelter the rear bulk material, which is kept at much lower temperatures, about 4-500 K lower. It is interesting to notice that ZrB_2-based samples not containing SiC did not show a sudden *temperature jump*, but rather a rapid increase in temperature already in the earliest stages of the test.

On the other hand, materials used as reference, i.e. graphite and C/SiC composites, together with Ti_3SiC_2-based samples demonstrated a considerable ablation rate, which made not possible reaching the most demanding conditions achievable with the UHTCMCs.

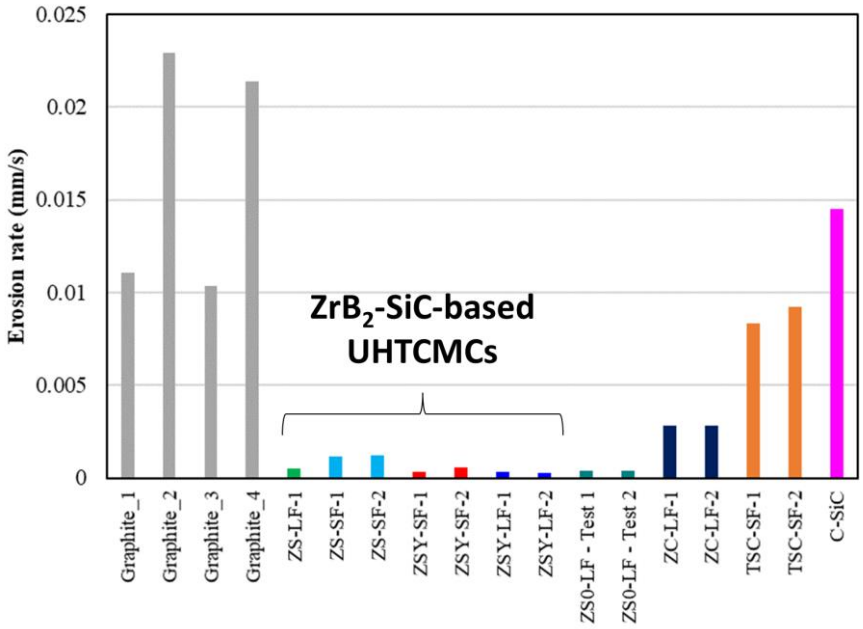

Fig. 5. Comparison of the ablation rates (based on mass loss) of the UHTCMC samples tested in SPES, showing the excellent ablation resistance of ZrB_2-SiC-based materials.

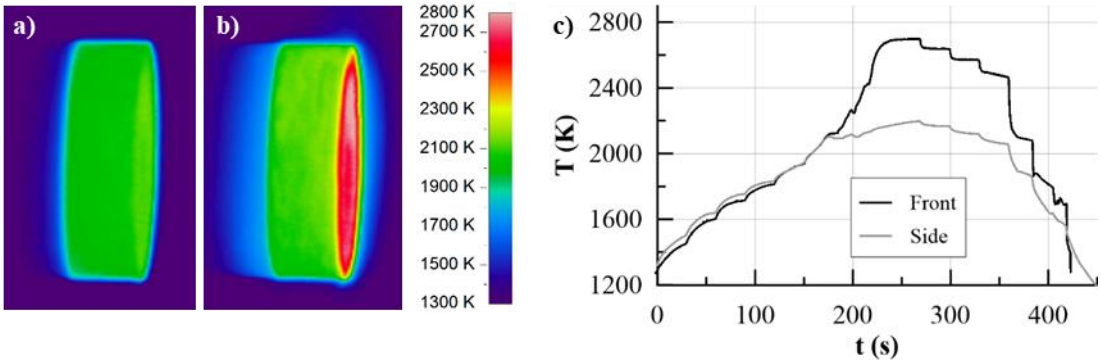

Fig. 6. Sample with ZrB_2-SiC matrix and long carbon fibres: Thermal images (a) before and (b) after the temperature jump, and (c) Comparison of temperature measured by ISQ5 pyrometer (front surface) and IGAR6 pyrometer (side surface).

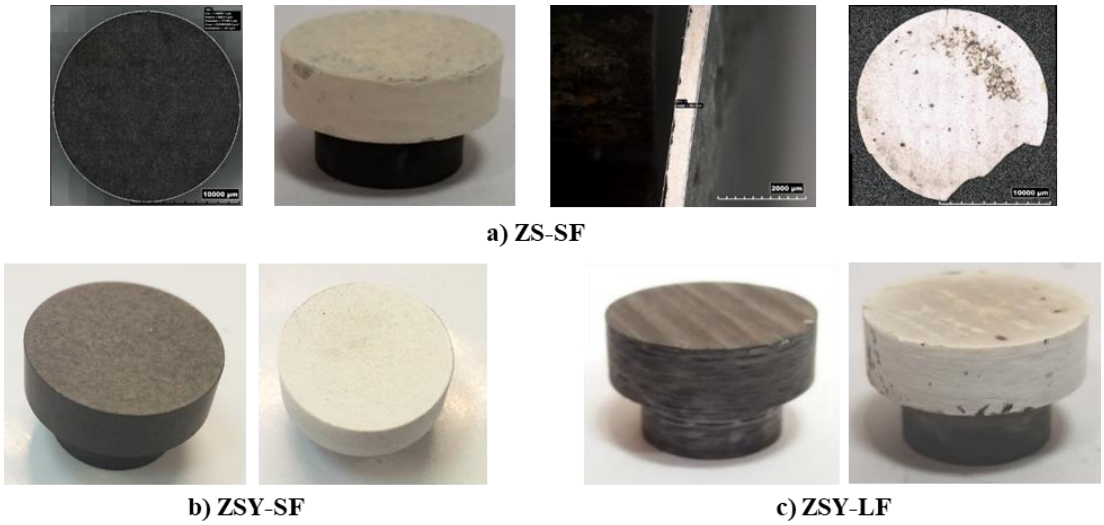

Fig. 7. Pictures of some samples before (left) and after (right) test. For sample ZS-SF-1 (a), pictures of the detached zirconia layer are also shown (the two pictures on the right).

To better investigate the phenomenon of the temperature jump, several further activities were carried out, studying the effect of SiC concentration in the original matrix [22] and oxygen partial pressure in the supersonic free-stream flow [23]. These results are not reported here in detail for the sake of brevity. However, the interpretation of the experimental results was complemented by post-test microstructural analyses (with the courtesy of CNR-ISTEC) and numerical CFD simulations.

The following observations were made:

- Jump occurs only on the front surface of the sample, when the temperature exceeds 2000-2300 K
- A liquid phase appears on the surface just before the jump (*waves-of-radiance* phenomenon)
- In presence of higher amounts of oxygen in the free-stream flow, jump is more retarded and gradual
- The jump is favoured by low SiC amount, but can occur for higher SiC content in case of longer exposure

Based on this, the phenomenon was related to the different stages of the ZrB_2-SiC UHTCs oxidation processes. The borosilicate glass (BSG) forming at relatively low temperature upon matrix oxidation melts at temperatures over 2000 K. If BSG replenishment in the outer oxide is not fast enough to counteract vaporization and shear stress transportation, a porous layer of ZrO_2 can be left exposed to the flow, being characterized by higher surface catalycity and lower thermal conductivity. Based on

these considerations, it was possible to perfectly match the temperature axial profile for one of the samples before and after jump, by CFD fluid-solid coupled simulations, as shown in Fig. 8 [24], taking into account an increased catalytic activity and reduced oxide thermal conductivity after jump.

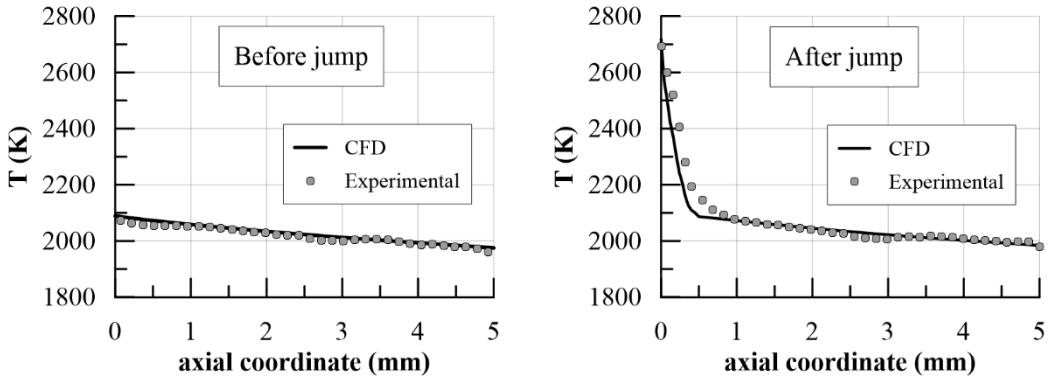

Fig. 8. Comparison between numerical and experimental temperature axial profiles, before (left) and after (right) temperature jump, for the same sample of Fig. 6.

3.2. UHTCMC for rocket nozzles

As described above, materials for rocket nozzles were tested according to an incremental approach, in four different test configurations. In the first one (free-jet tests), button-like samples were exposed to the supersonic plume coming out of the rocket nozzles. Materials with different matrix compositions and fibre architectures were compared in three different test conditions. Heat fluxes, estimated by CFD simulations [19] were in the order of 10-15 MW/m^2, at stagnation-point pressures up to 4 bar. The very stressful conditions caused most of the samples to consistently erode, experiencing a *temperature jump* which led the surface temperatures up to almost 3000 K (see Fig. 9). The sudden *temperature jump* was associated to a change in the shape of the flame surrounding the sample, as shown in the right part of the Figure. The only samples surviving the tests at 25 and 30 g/s mass flow rate were based on a ZrB2-SiC matrix and reinforced by continuous carbon fibres, demonstrating the good erosion resistance of this matrix composition, already validated in the re-entry environment. It is worth noticing that all the UHTCMCs presented an erosion rate considerably lower than a reference graphite sample (Fig. 10).

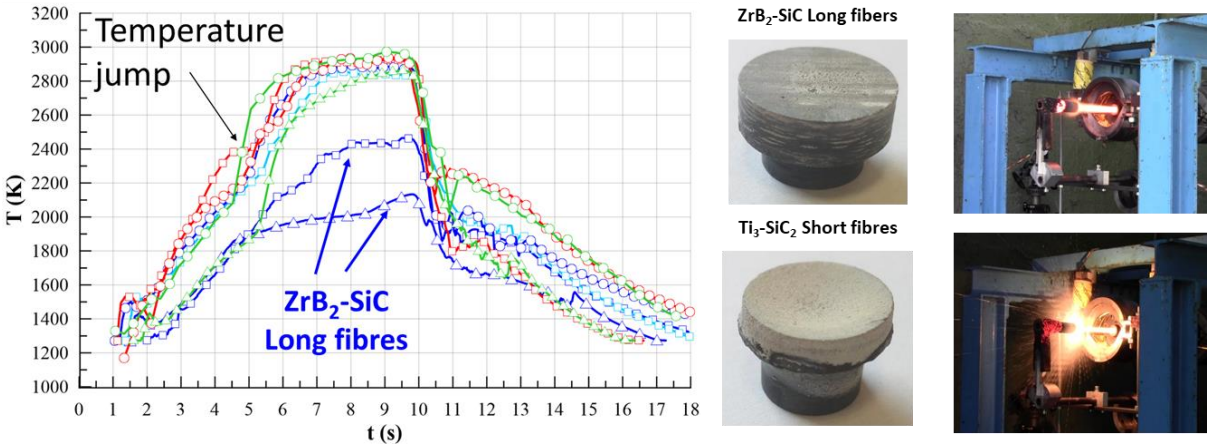

Fig. 9. Temperature histories of the samples tested in free-jet condition (left), two samples of different compositions after test (centre), corresponding frame of the test video, showing the occurrence of consistent erosion after temperature jump in the second sample (right).

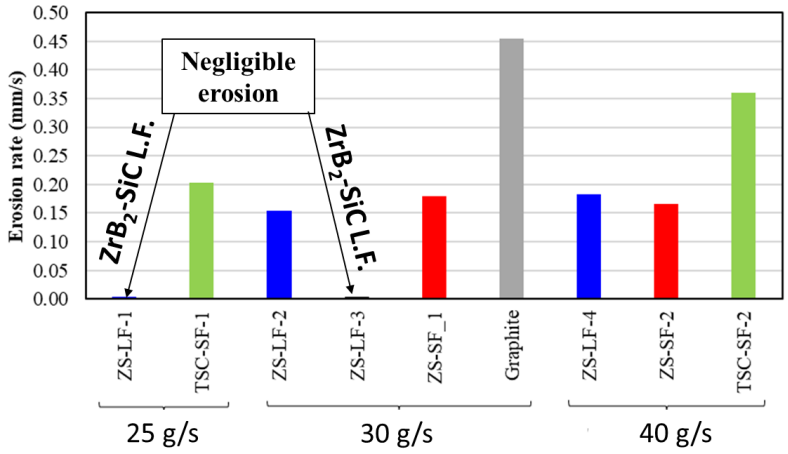

Fig. 10. Erosion rates of different free-jet samples. All UHTCMCs performed better than graphite, with long fibres ZrB_2-SiC-based UHTCMCs having almost negligible erosion in two test conditions.

Combustion chamber insert tests were conceived to characterize the UHTCMCs under high thermo-mechanical stress at high pressures (order of 10 bar) in relevant aerothermo-chemical combustion environment (at heat fluxes, estimated by CFD simulations on the order of 6-8 MW/m^2). A reference C/SiC sample provided by Airbus CRT was compared to long- and short-fibre reinforced ZrB_2-SiC-based materials, manufactured by CNR-ISTEC. As demonstrated by the post-test pictures of Fig. 11, the UHTC matrix demonstrated better erosion resistance than the conventional reference material, which moreover underwent surface delamination during engine disassembly. It could be also noticed that long fibres improved mechanical resistance, as expected, with respect to short fibres. The diverse behaviour of the chamber inserts can be ascribed to the thermal shock resistance of the starting material, i.e. in the case of the long-fibre samples, only when about 15% porosity was left after sintering no structural damage occurred. Accordingly, the material with short fibres (which provide weaker mechanical reinforcement), having a fully dense matrix and whose fibres integrity had been compromised during sintering, behaved as a brittle ceramic and shattered.

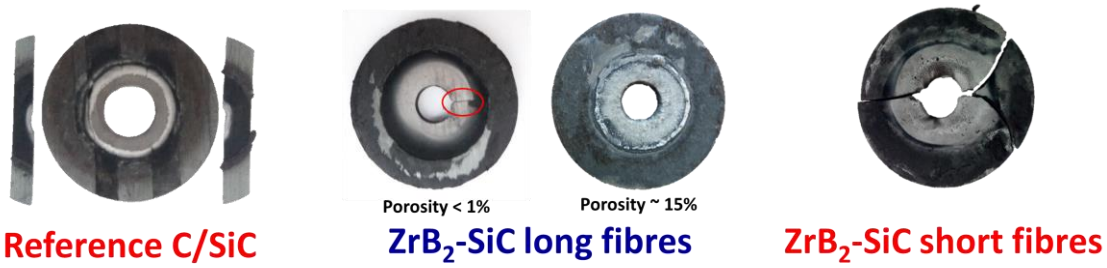

Fig. 11 Chamber inserts after tests.

Nozzle throat insert tests were used to characterize the materials in a condition much closer to a final application. Short- and long-fibres reinforced UHTCs, with ZrB_2-SiC matrix, were tested twice, at increasing oxidizer mass flow rates, 25 and 40 g/s, and correspondingly chamber pressure. A conventional graphite nozzle was also tested for comparison, showing an increase in the throat diameter from the initial 9.6 mm to 11.4 mm after two firings. On the contrary, the UHTCMCs displayed an excellent erosion resistance, especially the short-fibre one. The measured erosion rates are shown in the left part of Fig. 12. The different erosion behaviour is testified by the evolution of combustion chamber pressure, visibly decreasing over time in the case of graphite, as demonstrated by the right diagram of Fig. 12 (referred to the case at higher mass flow rate).

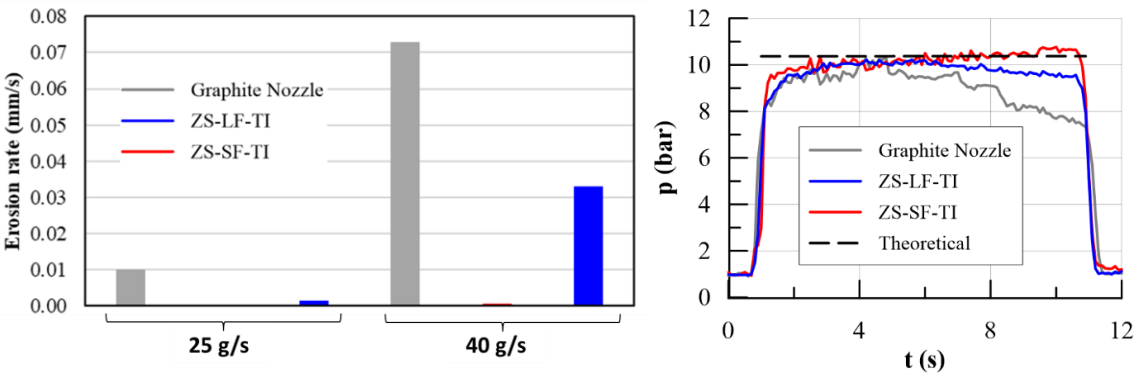

Fig. 12 Erosion rates of UHTCMC nozzle throat inserts (left), compared with graphite (red are short fibres, blue are long fibres), and corresponding pressure time profiles during tests at an oxidizer mass flow rate of 40 g/s (right).

The final test campaign was carried out on nozzles completely made of the UHTCMC material. Thirteen tests were performed in this configuration. Specifically, tests were carried out on three nozzles with ZrB_2-SiC matrix and long fibres, three nozzles with ZrB_2-SiC matrix and short (chopped) fibres, and one nozzle with a matrix based on ZrB_2 and pyrolytic carbon (PyC), with a 2.5D carbon fibre preform. Differences among the samples were also in the densification process, in the fibre volume content and the resulting material porosity. All tests were carried out at an oxygen mass flow rate of 40 g/s and some nozzles were subjected to repeated cycles to demonstrate reusability.

Fig. 13 shows the results on ZrB_2-SiC-based samples. All nozzles proved an excellent erosion resistance, as demonstrated by the stable profiles of combustion chamber pressure over time. As expected, long fibre reinforcement provided better mechanical performance, while an oversintered short-fibre nozzle underwent a catastrophic failure, resulting in gas leakage and decrease of chamber pressure. Post-test inspections revealed a radial crack departing from the sharp edge, which was likely the trigger for test failure. A combination of CFD and FEM analyses allowed estimating the thermal loads on the samples, the corresponding thermal distribution and a preliminary evaluation of the stress fields. Short-fibre nozzles have a relatively low thermal conductivity, which causes strong thermal gradients and accumulation of stress in the region where the crack originated, as shown by the results in the right part of Fig. 13. The ZrB_2-PyC-based nozzle was instead subjected to a strong erosion and structural damage, and the detailed results are not reported. Overall, the UHTCMCs demonstrated reusability over 2-3 cycles, for an overall test duration up to 30 s, demonstrating an excellent performance in a relevant small-scale environment at TRL close to 6.

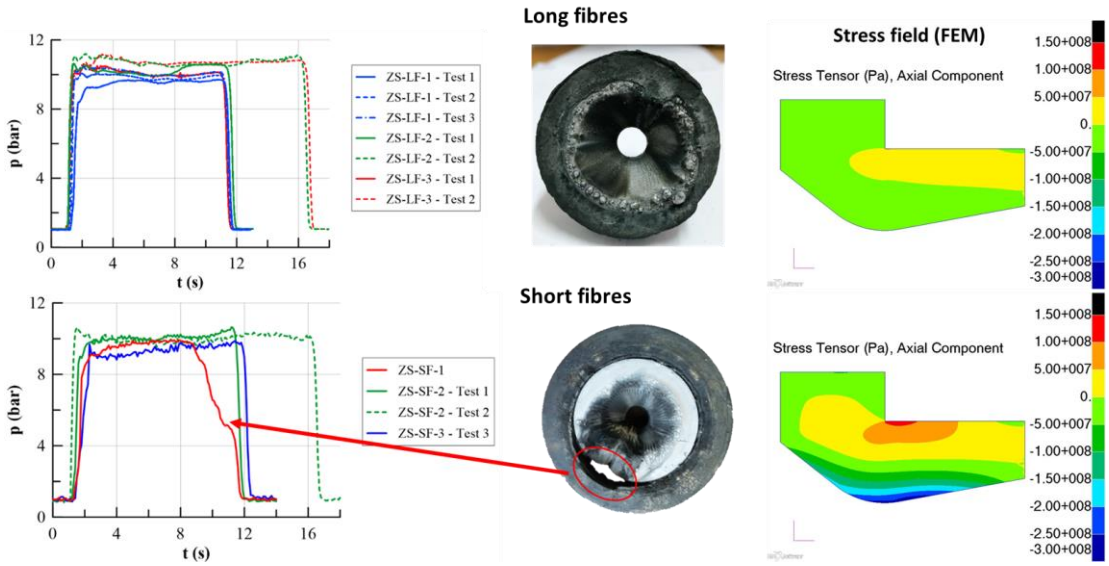

Fig. 13 Results of tests on complete UHTCMC nozzles (top: long fibres; bottom: short fibres): chamber pressure vs time for different tests (left), example picture after test (centre), results of structural simulations (right).

4. Conclusions and future developments

The work described in this paper was meant to provide a connection among different scientific and technological fields, and between industrial and research environments, in order to improve the understanding about UHTCs and UHTCMCs behaviour in relevant aero-thermo-dynamic environments. The collected data and the performed analyses contributed to the achievement of the goals of the C^{3}HARME project, which was successfully concluded, with a combined effort of the whole consortium, with the development and test of high-TRL large-scale prototypes (a complete TPS assembly tested in L3K, the hypersonic wind tunnel available at DLR in Cologne, and a large-scale solid rocket nozzle tested in AVIO test bench motors). The final objective of future research activities will need to include further increase of the TRL for the best performing materials, by a higher level of geometrical complexity, dimensions (up to full scale), system integration, and by all the necessary mechanical and environmental qualification assessments required by the space agencies for flight-ready space components. At present, a new collaboration is ongoing between UNINA and CNR-ISTEC, in a European Space Agency Announcement of Opportunity. The project is titled Wintertime and it is aimed at the characterization of ZrB2-SiC-based UHTCMC in a real space environment, by exposure to Low-Earth-Orbit outer space onboard the International Space Station.

In addition to the applications considered in the framework of C^{3}HARME, future research efforts could be interestingly devoted to assess and improve the performance of UHTCMCs in sharp TPS components, which would allow developing aerodynamically efficient wing leading edges for new-generation high-lift spaceplanes, able to perform controlled manoeuvres in extreme aero-thermo-dynamic conditions. Also, other applications such as TPS for planetary entry in space exploration missions (e.g. for Mars) or power generation (e.g. nuclear fusion plants, combustion chambers, solar panels) in ground- or space-scenarios will be of great interest, and specifically tailored development and testing would be needed.

Finally, several interesting developments may be considered from the modelling point of view, including more detailed rebuilding of thermal responses, taking into account the intrinsic anisotropy of composite materials, and possibly the dynamic simulation of oxidation and ablation processes.

Acknowledgements

The C^{3}HARME research project has received funding by the European Union's Horizon2020 research and innovation programme under the Grant Agreement n° 685594.

References

1. Fahrenholtz, W.G., Hilmas, G.E.: Ultra-high temperature ceramics: Materials for extreme environments. Scripta Materialia 129, 94-99 (2017)
2. Savino, R., Mungiguerra, S., Di Martino, G.D.: Testing ultra-high-temperature ceramics for thermal protection and rocket applications, Adv. Appl. Ceram. 117 (sup1), s9-s18 (2018)
3. Wuchina, E., Opila, E., Opeka, M., Fahrenholtz, W.G., Talmy, I.: UHTCs: Ultra-High Temperature Ceramic materials for extreme environment applications, Electrochem. Soc. Interface 16, 30-36 (2007)
4. Savino, R., Criscuolo, L., Di Martino, G.D., Mungiguerra, S.: Aero-thermo-chemical characterization of ultra-high-temperature ceramics for aerospace applications, J. Eur. Ceram. Soc. 38 (8), 2937-2953 (2018)
5. Evans, B., Kuo K., Cortopassi, A.: Characterization of nozzle erosion behavior under rocket motor operating conditions, Int. J. Energ. Mater. Chem. Propul. 9 (6), 533-548 (2010)
6. Hickman, R., Mc Kechnie, T., Agarwal, A.: Net shape fabrication of high temperature materials for rocket engine components, 37th Joint Propulsion Conference and Exhibit, Salt Lake City, UT, July 2001, AIAA paper 2001-3435
7. Johnston, J.R., Signorelli, R.A., Freche, J.C.: Performances of rocket nozzle material with several solid propellants, NASA technical note 3428.3 (1966)

8. Sanoj, P., Kandasubramanian, B.: Hybrid Carbon-Carbon Ablative Composites for Thermal Protection in Aerospace, J. Compos. 2014, 1-15 (2014)
9. Zheng, J., Cui, H., Lib, H., Li, Y., Yao, D., Ying, Z., Deng, H.: Mechanical and ablative properties of C/C composites modified by SiC using liquid silicon infiltration method, 68th International Astronautical Congress, Adelaide, Australia, September 2017
10. Kamps, L., Hirai, S., Ahmimache, Y., Guan, R., Nagata, H.: Investigation of Graphite Nozzle-Throat-Erosion in a Laboratory-Scale Hybrid Rocket Using GOX and HDPE, 53rd Joint Propulsion Conference and Exhibit, Atlanta, GA, July 2017, AIAA paper 2017-4736
11. Simonenko, E.P., Sevast'yanov, D.V., Simonenko, N.P., Sevast'yanov, V.G., Kuznetsov, N.T.: Promising Ultra-High-Temperature Ceramic Materials for Aerospace Applications, Rus. J. Inorg. Chem. 58 (14), 1669–1693 (2013)
12. Silvestroni, L., Kleebe, H.J., Fahrenholtz, W.G., Watts, J.: Super-strong materials for temperatures exceeding 2000°C, Sci. Rep. 7, 40730 (2017)
13. Parthasarathy, T.A., Petry, D., Cinibulk, M.K., Mathur, T., Mark, M.R., Gruber, R.: Thermal and Oxidation Response of UHTC Leading Edge Samples Exposed to Simulated Hypersonic Flight Conditions, J. Am. Ceram. Soc. 96 (3), 907-915 (2013)
14. Zhou, S., Li, W., Hu, P., Weng, L.: Ablation Behavior of ZrB_2–SiC–ZrO_2 Ceramic Composites by Means of the Oxyacetylene Torch, Corros. Sci. 51 (9), 2071-2079 (2009).
15. Purwar, A., Thiruvenkatam, V., Basu, B.: Experimental and computational analysis of thermo-oxidative-structural stability of ZrB_2–SiC–Ti during arc-jet testing, J. Am. Ceram. Soc. 100 (10), 4860-4873 (2017).
16. Tang, S., Hu, C.: Design, Preparation and Properties of Carbon Fiber Reinforced Ultra-High Temperature Ceramic Composites for Aerospace Applications: A Review, J. Mater. Sci. Technol. 33 (2), 117-130 (2017)
17. C3HARME Project Website: https://c3harme.eu/
18. Di Martino G. D., Carmicino C., Savino R., Transient Computational Thermofluid-Dynamic Simulation of Hybrid Rocket Internal Ballistics, J. Propuls. Power 33, 1395-1409 (2017)
19. Mungiguerra S., Di Martino G.D., Savino R., Zoli L., Silvestroni L., Sciti D., Characterization of novel ceramic composites for rocket nozzles in high-temperature harsh environments, Int. J. Heat Mass Transf. 163, 120492 (2020)
20. Di Martino G. D., Mungiguerra S., Cecere A., Savino R., Vinci A., Zoli L., Sciti D., Hybrid rockets with nozzle in ultra-high-temperature ceramic composites, IAC-18.C4.3.6x47333, 69th International Astronautical Congress, Bremen, Germany, 2017
21. Di Martino G. D., Mungiguerra S., Carmicino C., Savino R., Cardillo D., Battista F., Invigorito M., Elia G., Two-Hundred-Newton Laboratory-Scale Hybrid Rocket Testing for Paraffin Fuel-Performance Characterization. J. Propuls. Power 35, 224-235 (2019)
22. Mungiguerra S., Cecere A., Savino R., Saraga F., Monteverde F., Sciti D., Improved aero-thermal resistance capabilities of ZrB2-based ceramics in hypersonic environment for increasing SiC content, Corros. Sci. 178, 109067 (2021)
23. Silvestroni L., Mungiguerra S., Sciti D, Di Martino G.D., Savino R., Effect of hypersonic flow chemical composition on the oxidation behavior of a super-strong UHTC, Corros. Sci. 159, 108125 (2019)
24. Mungiguerra S., Di Martino G.D., Cecere A., Savino R., Zoli L., Silvestroni L., Sciti D., Ultra-High-Temperature Testing of Sintered ZrB2-based Ceramic Composites in Atmospheric Re-entry Environment, Int. J. Heat Mass Transf. 156, 119910 (2020)